Available online at www.sciencedirect.com
SCIENCE DIRECT®
International Journal of Mass Spectrometry 228 (2003) 825–839
International Journal of Mass Spectrometry
www.elsevier.com/locate/ijms

Na^+ affinities of gas-phase amino acids by ligand exchange equilibrium

Alexei Gapeev, Robert C. Dunbar*

Chemistry Department, Case Western Reserve University, 2N Millis Science Center, 10900 Euclid Avenue, Cleveland, OH 44106, USA

Received 5 February 2003; accepted 2 April 2003

Dedicated with utmost admiration and friendship to Helmut Schwarz in celebration of his 60th birthday.

Abstract

Ligand exchange equilibrium in the Fourier-transform Ion Cyclotron Resonance ion trap was used to compare Na^+ ion attachment free energies of the amino acids Gly, Ala, Val, Pro, Cys, Ser, Asn, His, Phe, and Trp, along with the reference compounds pyridine (Pyr), methylalanine (MeAla), and methylvaline (MeVal). Attachment entropies were estimated, including dynamical and conformational components, and the free energies were converted to attachment enthalpies (Na^+ affinities). The results were compared with those from a concurrent study [Int. J. Mass Spectrom. (2003) in press] using the "kinetic method" of competitive ligand dissociation. For Gly, Val, Cys, Ser, Phe, and Trp, the affinities relative to Ala from these two methods are in good agreement, and are also in accord with available theoretical estimates. The Na^+ affinity of Pro from equilibrium attachment is lower by 20 kJ mol^{-1} than that from kinetic method detachment. This is believed to reflect the fact that neutral gas-phase Pro has a preferred non-zwitterionic structure, whose Na^+ affinity is lower than the zwitterionic form which is presumed to be formed in the electrospray source used in the kinetic method experiment. The affinity of His from the present study is lower by 35 kJ mol^{-1} than the kinetic method study, and it is speculated that this might reflect a predominance of the low-affinity tautomer of His in the gas phase. Considering the present results (anchored to a literature value for Pyr) and other recent experiments, we agree with Kish et al.'s assignment of the absolute affinity of Gly as 161 ± 8 kJ mol^{-1} for the absolute anchoring of the affinity scale. New DFT/B3P86 computations of the affinities of these amino acids (as well as Asn) are reported, and compared with experiment.

Keywords: Sodium ion affinity; Amino acids; Equilibrium; FT-ICR

1. Introduction

The binding of sodium ions to amino acids has interest in several ways. This is a readily available series of molecules having a degree of commonality of the metal-attachment sites, but also having a variety of metal-chelation motifs involving the various side chains. As such, they offer an attractive domain for exploring the thermochemistry and the geometries of ion binding by oxygen and nitrogen (and sulfur) in highly chelating complexes. Being small enough for chemically meaningful computational study of the

* Corresponding author. Tel.: +1-216-368-3712; fax: +1-216-368-3006.
E-mail address: rcd@po.cwru.edu (R.C. Dunbar).

1387-3806/$ – see front matter © 2003 Elsevier Science B.V. All rights reserved.
doi:10.1016/S1387-3806(03)00242-2

complexes along with detailed gas-phase characterization of the binding, they are useful models for exploring the interplay of non-covalent binding energies, energies of geometrical distortion, and entropic factors, in determining the nature of an equilibrium population of sodium-complexed molecules. Moreover, although the bare amino acids themselves have limited direct interest as biological sodium ion carriers, understanding gained about the nature and thermodynamics of binding to their numerous electron-rich sites carries over to thinking about sodium ion binding to more biologically relevant sites offered at the surfaces of oligopeptides and proteins.

Numerous groups have given recent attention to these systems with a variety of experimental and computational approaches. A study of Na^+ affinities using the kinetic method (which analyzes the competitive dissociation of heterodimers $R_1R_2Na^+$) was carried out by Kish et al. [1] at the same time as the present experiments, and provides a particularly useful point of comparison. The kinetic method looks at dissociation of Na^+ complexes pre-formed in an electrospray source. In contrast, the ligand transfer equilibrium experiment looks at the attachment of Na^+ to ambient neutral amino acids in the gas phase. One might expect to find informative differences in the results of these two methods, corresponding to their very different routes of formation of the sodium complexes.

McMahon and coworkers have applied the equilibrium approach to the determination of Na^+ affinities of a wide variety of ligands, most recently reported in Ref. [2], but the low volatility of the amino acids makes them difficult targets which have not yet been reported. Here, we report the successful application of this approach for a number of amino acids.

The thermodynamics of ion attachment concerns not only the nature and strength of the ion-bound complex, but also the nature of the neutral molecules on the ion-detached side of the reaction. The neutral amino acids at room temperature have a challenging richness of thermodynamic possibilities, because their numerous possible intramolecular hydrogen-bonding motifs, along with the presence of numerous internal-rotational variations, lead to a number of thermally accessible conformers. The number, energies, and interconversions of these conformers are not well characterized for most cases. Some experimental progress about gas-phase thermal conformer distributions has been gathered by sorting out spectroscopic observations of thermal populations for a few of the smallest cases, as for instance, the microwave, [3] electron diffraction [4], and photoelectron spectra [5] of alanine. Also promising is a new approach via dipole moment measurements [6]. Measurements of equilibrium ion attachment carry information about the thermal distribution of conformers through the entropy of complexation, and could make future contributions to the question of conformer distributions, but we are still far from being able to measure the entropies of attachment with sufficient precision to make progress in this direction. For most cases, the best information about neutral amino acid conformer distributions is still that coming from computations, and it is computational results that we have chosen to draw on for the conformer distributions needed in the present work.

The low volatility of the amino acids makes it challenging to reach and maintain a sufficient pressure for equilibrium studies, even though Fourier-transform Ion Cyclotron Resonance (FT-ICR) equilibrium studies are feasible with sample pressures even below 10^{-9} Torr. The amino acids described here have been found to be sufficiently volatile for success in our apparatus. Several others (Arg, Lys, Asp) were considered interesting and potentially feasible, but attempts to volatilize these by heating the solid-insertion probe gave decomposition before any observable sample vapor was produced.

2. Methods

2.1. Experimental

Equilibrium determinations were made using the Nicolet FT-2000 mass spectrometer with a 3 T magnet, operated with an IonSpec Omega data system, as used in previous experiments [7,8]. Setups and procedures

were generally similar to the previous study reported for Ala and Phe [8].

The amino acid was introduced into the chamber on the solid-insertion probe, and its pressure was brought to an appropriate working level by raising the temperature of the entire vacuum chamber. After thorough stabilization and equilibration of the pressure, the sample pressure was measured as before [8] using the proton transfer reaction from propyl cation. The three compounds used as reference partners (pyridine (Pyr), *o*-methylalanine (MeAla), and *o*-methylvaline (MeVal)) were introduced through the leak valve. The reference gas pressure was monitored by the ionization gauge, calibrated for each reference compound against the propyl cation proton transfer reaction. Na^+ ions were readily produced by laser desorption (Nd:YAG laser at 1064 nm) from a piece of NaCl mounted on the solid-insertion probe.

Fig. 1 shows a typical set of time plots for the approach to equilibrium (illustrated for Ser equilibrated with MeVal). Fig. 1a shows the experiment in which all ions in the ICR cell except the $MeValNa^+$ ion are ejected at time zero, and the subsequent relaxation toward equilibrium is observed, corresponding to the forward direction of the equilibrium reaction

$$MeValNa^+ + Ser \rightleftarrows SerNa^+ + MeVal \quad (1)$$

(The initial laser pulse producing Na^+ occurs several seconds prior to the zero of time on the figure, so that by time zero most of the Na^+ has attached to one of the neutral species present in the cell.) The corresponding reverse experiment shown in Fig. 1b is initiated at time zero by ejecting all ions except $SerNa^+$ at time zero, and observing the approach to equilibrium from the other side, according to Eq. (1) proceeding in the reverse direction. In this figure, both the forward and reverse experiments are fitted to exponential relaxation curves, with equilibrium values of 0.775 and 0.225 for the fractions of $SerNa^+$ and $MeValNa^+$, respectively. This equilibrium peak ratio is then converted to the equilibrium constant by dividing by the ratio of neutral pressures. (It can be seen in Fig. 1a that the first point, at time zero, does not fit the relaxation kinetic curves. This probably reflects a situation where the cyclotron ejection pulse at zero time leaves the $MeValNa^+$ ions with significant kinetic excitation, which is only dissipated by several ion–neutral collisions. Thus, the transfer of Na^+ to Ser is inhibited for the first second or so, and the exponential relaxation kinetics are only followed after this initial period of kinetic energy dissipation.)

Table 1 shows experimental parameters for all the experiments, and indicates the resulting equilibrium constant results in the form of $\Delta G^\circ_{eq,\,T}$ values for Na^+

Table 1
Experimental parameters for the experiments, and $\Delta G^\circ_{eq,\,T}$ values derived from the equilibrium observations (ΔG° of transfer of Na^+ from reference molecule to amino acid, kJ mol^{-1})

Amino acid	Reference molecule	T (K)	P (amino acid)[a]	P (reference)[a]	$\Delta G^\circ_{eq,\,T}$
Ala[b]	Pyr	326			−20.9
Ala[b]	MeAla	370			9.6
MeAla[b]	Pyr	370			−30.1
Gly	Pyr	298	1.4(−7)	3.5(−6)	−15.1
Val	MeAla	298	6.0(−9)	7.2(−9)	5.0
Cys	MeVal	353	3.0–7.0(−8)	8.0(−9)	3.6, 3.1
Pro	MeAla	353	1.0(−8)	4.7(−8)	−1.3
Asn[c]	MeAla	343	4.0(−9)	3.5(−8)	(<−2.8)[c]
Ser	MeVal	368	3.2(−8)	2.4(−8)	−3.3
His	MeVal	393	3.0(−8)	1.2(−7)	−5.9
Phe[b]	MeAla	370			−13.8
Trp	MeAla	393	1.1(−8)	5.0(−7)	−20.1

[a] Pressures in Torr (exponents in parentheses).
[b] Experiments and results described in Ref. [8].
[c] Equilibrium was not established, so this free energy of transfer is only an upper limit.

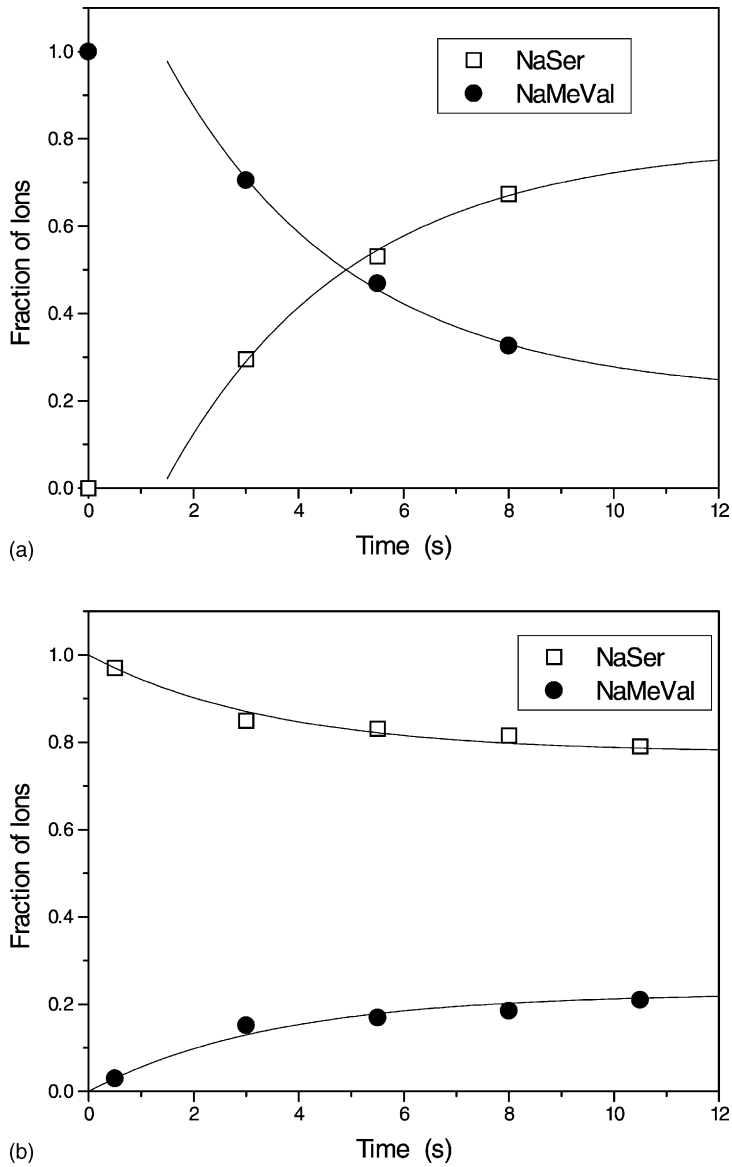

Fig. 1. Time plots showing the approach to equilibrium in both directions for the $SerNa^+$ system. (a) Reaction starting with isolated $MeValNa^+$ ions. (b) Reaction progress starting with isolated $SerNa^+$ ions. See Table 1 for details.

transfer from reference molecule to amino acid, as derived from the equilibrium constants.

2.2. Computational

The computational protocol was based on Density Functional (DFT) calculations using the B3P86 functional, which has been considered to be particularly accurate for sodium ion affinities [9]. Structures were optimized and vibrational frequencies were calculated using a basis set consisting of 6-31+g(d,p) on the amino acid atoms, and 6-311+g(d) on Na. Final energy calculations used an expanded basis of 6-311+g(2df,2pd) on all atoms. Binding energies were

Table 2
Computed Na^+ affinities (enthalpy of Na^+ detachment) using the present computational protocol (kJ mol^{-1})

	Uncorrected	−ZPVE	−BSSE	Affinity[a]
Gly	168.9	7.1	2.1	159.7
Ala	174.7	6.7	1.8	166.2
Cys	177.9	5.0	2.4	170.5
Pro	197.8	6.7	1.8	189.3
Asn	217.5	3.8	2.6	185.9
Ser	195.4	6.7	2.6	186.2
His	233.5	5.4	2.4	225.7
Phe	197.9	6.7[b]	2.9	188.3
Trp	225.9	7[b]	4	214.9
Pyr[b]	134	4	1	129[b]
MeAla	184.5	7.5	2.3	174.7
MeVal	188.3	7.2	2.9	178.2

[a] Including ZPVE and BSSE corrections. These are 0 K values. In Table 8, they have been corrected to 298 K using the computed thermal energies. For approximate conversion between 0 and 298 K, note that the thermal correction from 0 to 298 K is consistently found to lie in the range 2 ± 1 kJ mol^{-1}.
[b] Ref. [8].

corrected as shown in Table 2 for zero-point vibrational energy (ZPVE) effects, and for basis set superposition errors (BSSE) using the geometry-consistent approach described by Xantheas [10]. Trp was too large for this basis set, and a reduced basis was used, with 6-311+g(df,pd) on the amino acid atoms and 6-311+g(2df,2pd) on Na.

3. Computational results and data analysis

3.1. Entropy corrections

3.1.1. Dynamical entropy

The vibrational, rotational, and translational contributions to the entropy of dissociation were calculated in the rigid-rotor-harmonic-oscillator approximation. Although the larger amino acids have various possibilities for the hindered internal rotors, it can be hoped that these will be adequately taken care of in the form of multiple conformers in the conformational entropy calculation.

3.1.2. Conformational entropy

The numerous hydrogen-bonding motifs available to neutral amino acids lead to a substantial number of low-energy conformations. If these are in communication with each other without substantial barriers, or if they are available as dissociation products of the complex, then there is a conformational contribution to the entropy of dissociation which affects the ΔG° of dissociation. The conformational entropy is easily evaluated by summing the contributions to the partition function

$$q = \sum_i q_i \exp\left(-\frac{\varepsilon_i}{kT}\right) = q_i \sum_i \exp\left(-\frac{\varepsilon_i}{kT}\right), \qquad (2)$$

where the sum is over all communicating conformations, ε_i is the energy of the conformation relative to the lowest one, q_i is the individual partition function of each conformation, and the last equality assumes that the q_i's are equal. Then, the conformational entropy comes from the standard equation

$$S = \frac{1}{qT}\sum_i \varepsilon_i \exp\left(-\frac{\varepsilon_i}{kT}\right) + R \ln q. \qquad (3)$$

It is likely that the various low-lying internal-rotational conformers of the amino acids will be accessible thermally as well as being available as dissociation products of the complex, so it seems appropriate to include all of them in the statistical-thermodynamic evaluation of the entropies. Conformers lying within roughly 5 kJ mol^{-1} of the lowest one contribute substantially to the entropy, and most of the amino acids have multiple conformers meeting this criterion. It is not easy even to enumerate all of the relevant conformers: For instance, the number of assigned low-lying Ala conformers has increased substantially in recent work, progressing from Ref. [3] to Ref. [11] to Ref. [12]. On the other hand, the structure-constraining effect of the chelated metal ion generally leads to a unique low-energy conformation of the metal–ion complex. (Val, in which the side chain is not constrained by chelation, is the only case here where conformational entropy contributions to the complex are likely to be significant.) Accordingly, the present allocations of conformational entropies will assume a single conformer for the Na^+ complexes, but will give some consideration to evaluating and estimating

the entropy contributions appropriate for the neutral amino acids.

Present computational methods are not sufficiently accurate to characterize the relative energies of the different low-energy conformers within the accuracy of the order of 1 kJ mol^{-1} that would be required to make convincingly accurate calculations of the conformational entropies. However, the relative energetics can be calculated within a few kJ mol^{-1} accuracy, which is sufficiently good to make useful assessments of the likely entropy contributions. Interestingly, when comparisons are made of various conformational studies that have been reported for some of the simpler amino acids, it is found that the relative energies, and even the ordering, of the conformers change drastically depending on the computational method and level. However, the different approaches generally give a similar number and spacing of conformers in the low-energy range (up to 6 or 8 kJ mol^{-1}). Typically, a half dozen conformers are distributed in this important low-energy region. Accordingly, it seems possible to make reasonable estimates of the conformational entropies of the amino acids in the relevant temperature region, even though we would have no confidence in the detailed ordering and spacing of the conformers predicted by any particular conformer-comparing study at presently accessible levels of computational accuracy.

The conformational entropies used are summarized in Table 3. The study of Ala, Ser, and Cys by Gronert and O'Hair [11] found comprehensive sets of conformers for these cases, and these were adopted for the entropy assignments. Siu's assignment [13] for Ser gave a slightly lower entropy, and that for Cys was lower by a substantial 10 J K^{-1} mol^{-1}, but it is not certain that their conformer assignments were comprehensive. The set assigned by Császár [12] for Ala gave a similar entropy to that of Gronert and O'Hair. For Gly, the set of conformers found by Császár [14] was adopted, which is similar to that given by Siu [13].

Val was assigned the same entropy as Ala. This is possibly incorrect, since the three rotational orientations of the isopropyl group may be thermally accessible. However, such an entropy would likely be canceled by a similar entropy contribution for the ValNa$^+$ complex, which was also ignored. This uncertainty also arises in considering the MeVal entropy. The uncertainty is of the order of 10 J K^{-1} mol^{-1}, which adds an uncertainty of up to 3 kJ mol^{-1} in the thermochemistry of Val and MeVal complexation.

Table 3
Entropy of dissociation of MNa$^+$

	$\Delta S^\circ_{\text{dyn, 298}}$	$\Delta S^\circ_{\text{conf, 298}}$	$\Delta S^\circ_{\text{tot, 298}}$
Gly	116.7	8	125
Ala	117.2	13	130
Val	(117)	(13)	130
Cys	114.2	16	130
Pro	109.2	9	118
Asn	111.3	8	119
Ser	123.3	13	136
His	113.0	(8)	121
Phe	126*	18*	144
Trp	(126)	(18)	144
MeAla	117.2	(5)	122
MeVal	117.7	(5)	123
Pyr	98.5	0	98.5

$\Delta S^\circ_{\text{dyn, 298}}$ is the contribution of rotation, vibration, and translation, $\Delta S^\circ_{\text{conf, 298}}$ is the conformational contribution, and $\Delta S^\circ_{\text{tot, 298}}$ is the net entropy of dissociation (J K^{-1} mol^{-1}).
Values in parentheses are estimated with limited confidence. Values marked (∗) are based on Ref. [8]. All values are calculated at 298 K. A model calculation on Cys suggested that $\Delta S^\circ_{\text{tot}}$ increases by ∼10% for each increase of 30 K above 300 K, and this was used as a guide to estimating temperature dependences of the $\Delta S^\circ_{\text{dissoc}}$ terms.

The entropy of neutral His is a complex question which was not addressed seriously here. The two tautomers of neutral His presumably do not interconvert thermally. At the present level of computation, these two tautomers have exactly equal energies. Some discussion of the possible significance of the existence of the two tautomers for the present results is given below.

A survey of the low-energy conformers of neutral Asn was carried out, and will be described in detail elsewhere. The lowest five conformers found in the search were calculated with our full DFT protocol, as displayed in Table 4, which is believed to include all the conformers lying within about 10 kJ mol^{-1} of the lowest. The lowest neutral conformer is the compact, highly H-bonded structure shown in Fig. 2. The dissociation entropy of this complex is calculated to be

Table 4
Computed relative energies of the lowest conformers of Asn

H-bonding interactions[a]	Energy (kJ mol^{-1})
OH/N_A, HN_A/O_S, HN_S/O_A	0
OH/N_A, HN_A/O_S	3.8
OH/O_S, HN_A/O_A	4.0
OH/O_A, HN_A/O_A, HN_S/N_A	8.0
OH/N_A, HN_S/O_A	8.2

[a] OH, O_A, and N_A refer to the amino acid hydroxyl, carbonyl, and amine groups, respectively, and O_S and N_S refer to the side chain carbonyl and amino groups, respectively.

relatively low, as indicated in Table 3, both because the structure shown in Fig. 2 is substantially more stable than the alternatives, and also because its compact structure leads to a low dynamical entropy.

Siu [13] and Császár and Perczel [15] listed conformation sets which give similar entropies for Pro.

Some estimation of the conformational entropy of Phe was made in Ref. [8], and no further consideration was made here. No attempt was made to calculate entropy contributions for Trp, and the estimates given in Table 3 for this system are assigned by analogy with Phe.

The net entropies of dissociation are given in Table 3, and were used in the data reduction in the next section. The dynamical entropy contributions for Gly, Ala, Pro, and Ser are in good agreement with those calculated in Ref. [1], but those authors did not include conformational entropy contributions, making their net entropies somewhat low. The present dynamical entropy contribution calculated for Cys is 10 J K^{-1} mol^{-1} lower than theirs, probably reflecting different vibrational frequencies from the different computational approaches.

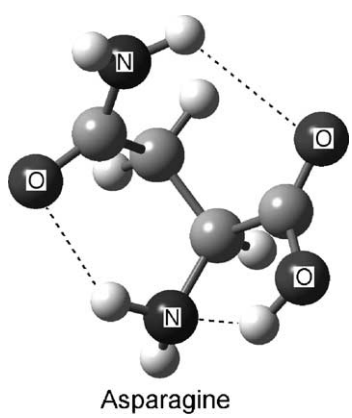

Fig. 2. The highly H-bonded structure which is the most stable conformer of neutral Asn.

3.2. Data reduction from ΔG to ΔH

The equilibrium measurements displayed in Table 1 were made at various temperatures, using three different reference partners. The steps to bring all the results to a common basis were: (1) reduce all $\Delta G^\circ_{\mathrm{eq},T}$ measurements to 298 K; (2) reduce all values to relative ΔG°_{298} of sodium ion transfer to Ala at 298 K; (3) convert the relative ΔG°_{298} values to relative ΔH°_{298} of transfer to Ala. These steps are summarized in Table 5, and outlined below:

(1) First, all experimental $\Delta G^\circ_{\mathrm{eq},T}$'s were corrected to 298 K. It was assumed that there were no differential enthalpy effects, so that ΔH of transfer from reference molecule to amino acid was the same at 298 K as at the equilibration temperature. As a first approximation, one similarly expects no differential ΔS effects. Actually, the entropy calculations show that ΔS° of dissociation increases slowly with increasing T, leading to a temperature dependence of the ΔS° of dissociation. These effects are of the order of 10 or 20% over the temperature range of interest here. This has a very small effect on the results, but for correctness, the entropy values used in making this correction were not exactly the ΔS°_{298} values given in Table 3, but rather the values averaged over the range from 298 K to the temperature of equilibration. The values of ΔS°_{298} of transfer from reference base to amino acid were estimated at two temperatures in order to make this temperature-averaging correction to the 298 K values in Table 3. Explicitly, the approximate equation used for the temperature correction of the ΔG°'s is

$$\Delta G^\circ_{298} = \Delta G^\circ_{\mathrm{eq},T} + (T - 298)\Delta S^{\circ,\mathrm{av}}, \qquad (4)$$

Table 5
Reduction of $\Delta G^{\circ}_{eq,\,T}$ (from Table 1) to ΔH°_{298} relative to Ala

Molecule	Reference	T	ΔG°_{298}	ΔG°_{298} vs. Ala[a]	ΔH°_{298} vs. Ala[a]
Pyr	Ala	326	21.7	21.7	31.1
MeAla	Ala	370	−9.0	−9.0	−6.6
MeAla	Pyr	370	−30.8	−9.1	−6.7
Gly	Pyr	298	−15.1	6.6	8.1
Val	MeAla	298	+5.0	−4.0	−4.0
Cys	MeVal	353	+2.9	−9.6	−9.6
Pro	MeAla	353	−1.1	−10.1	−6.5
Asn	MeAla	343	(<−0.7)	(<−9.7)	(<−6.1)
Ser	MeVal	368	−4.3	−16.8	−18.6
His	MeVal	393	−5.7	−18.2	−15.5
Phe	MeAla	370	−15.6	−24.6	−28.8
Trp	MeAla	393	−22.6	−31.6	−35.8

[a] ΔG°_{298} or ΔH°_{298} of transfer from Ala to the specified molecule (kJ mol^{-1}).

where $\Delta S^{\circ,\,av}$ is the average ligand transfer entropy over the temperature range.

(2) Second, all ΔG°'s were referred to Ala. For the cases using MeAla as the reference, this was done via the previously assigned ΔG° of Na^+ transfer from Ala to MeAla of $-9.6\,kJ\,mol^{-1}$ at 370 K, adjusted to $-9.0\,kJ\,mol^{-1}$ at 298 K. In the case of Gly, for which the reference base was pyridine, this was done via the previously assigned ΔG°_{298} of Na^+ transfer from Pyr to MeAla of $-15.1\,kJ\,mol^{-1}$.

For the cases where the reference was MeVal, it was necessary to assign a ΔG° of transfer between MeVal and MeAla. The ΔH° part of this was calculated by comparing the DFT energies of Na^+ detachment. This calculation gave a ΔH°_{298} of transfer of Na^+ between the most stable conformers of MeAla and MeVal as $-3.5\,kJ\,mol^{-1}$. The dynamical ΔS° contributions for MeVal to MeAla transfer were taken to be zero, on the assumption that the vibrational and other dynamical entropies of Na^+ attachment would be similar for these two similar molecules and complexes. The possibility of a conformation entropy effect on this transfer was also considered: There are three conformers of MeVal corresponding to the rotation of the isopropyl side chain, and a corresponding set of three conformers of MeValNa^+. The less stable conformers are calculated to lie within less than $5\,kJ\,mol^{-1}$ of the most stable ones for both neutral and complex, so that it is probably impossible to make an accurate calculation of the conformational entropy contribution to the Na^+ transfer. It is expected that the conformational entropies of the neutral and the complexed Val species will largely cancel out, and these effects would not in any case give an effect of more than 1–2 kJ mol^{-1}, so this possible conformational contribution was ignored. Thus, the entropy of Na^+ transfer was set equal to zero, and ΔG°_{298} (and also ΔH°_{298}) of Na^+ transfer from MeVal to MeAla was assigned as $3.5\,kJ\,mol^{-1}$.

(3) The ΔG°_{298}'s of transfer were converted to ΔH°_{298}'s by subtraction of the $T\Delta S$ terms. Since this conversion is at 298 K, the entropies of Table 3 could be used without temperature corrections.

3.3. Most stable structures and conformations

3.3.1. Neutrals

Studies have been described at a good computational level of the structures and low-lying conformers of Gly, Ala, Pro, Ser, Phe, and Cys (see Refs. [13,15] for recent summaries). These were not studied further here beyond optimizing and computing the previously assigned lowest energy conformer with the present computational protocol.

The geometry of neutral Trp was considered in our previous work [16], from which the lowest energy conformation has been taken and recalculated, using a somewhat reduced basis from the rest of the present study.

As discussed below, the two tautomers of His are both of interest. There are numerous low-lying conformers, which were not extensively characterized, beyond a search for the most stable conformers at the Hartree–Fock/3-21g level. The most stable conformer of each tautomer was optimized with the present computational protocol, giving identical energies for the two tautomers. This is a notable contrast to the situation for the zwitterion structures that are stable in condensed phase: for the zwitterions, the $N^{\varepsilon 2}$–H tautomer is much more stable [17].

3.3.2. Complexes

Most of the Na^+ complexes have a lowest energy structure which is clearly better than the alternatives. Of those of interest here, all of the complexes are accepted to be charge-solvated structures (as opposed to zwitterions), with the exception of $ProNa^+$ whose most stable structure is the sodiated zwitterion with

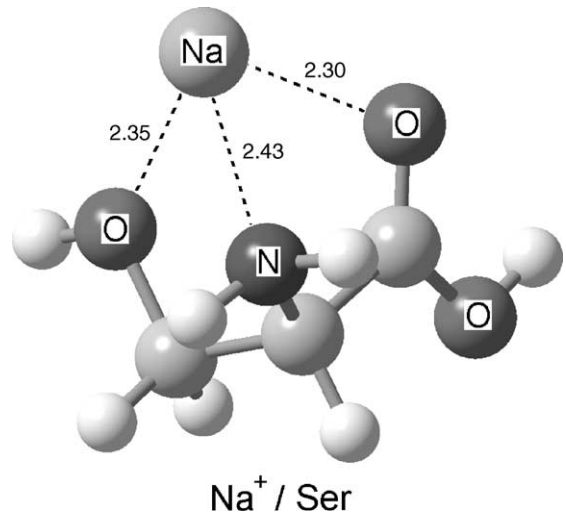

Fig. 4. Structure of the most stable form computed for the $SerNa^+$ complex.

complexation to the two oxygens. The aliphatic amino acids have bidentate complexation using the nitrogen and the carbonyl oxygen. The side chains of the others contain potentially chelating groups, and in fact all of them form threefold chelated complexes. These are shown in Figs. 3–6 for Cys, Ser, His, and Asn. Fig. 7

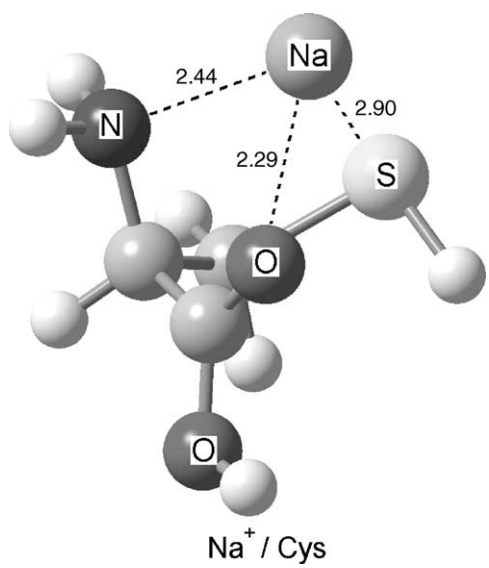

Fig. 3. Structure of the most stable form computed for the $CysNa^+$ complex.

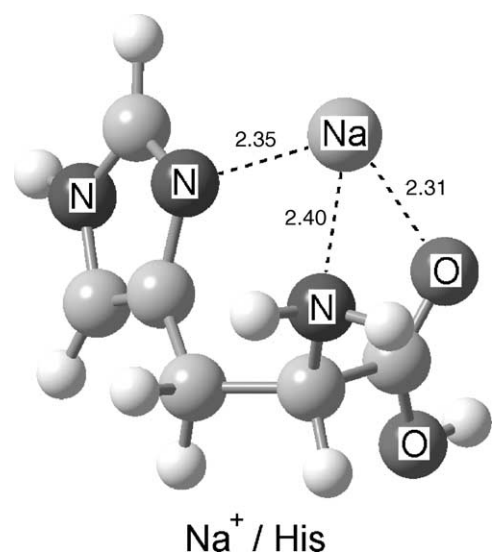

Fig. 5. Structure computed for the $HisNa^+$ complex in the most stable $N^{\delta 1}$ tautomeric form.

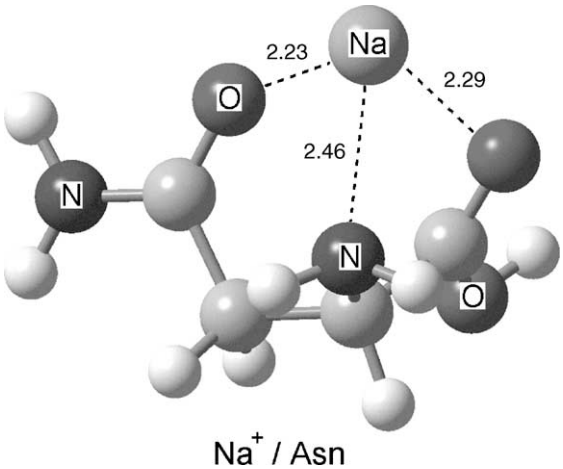

Fig. 6. Structure of the most stable form computed for the AsnNa$^+$ complex.

shows the zwitterion complex of Pro, and Fig. 8 shows the most stable of the possible non-zwitterionic conformers of ProNa$^+$ [13]. We have described the complexes of the pi-chelating amino acids Phe and Trp previously [8,16].

HisNa$^+$ has the complication that either of the two His isomers can form chelated Na$^+$ complexes. However, the N$^{\delta 1}$-chelated isomer shown in Fig. 5 chelates with much less strain, and is calculated to be more

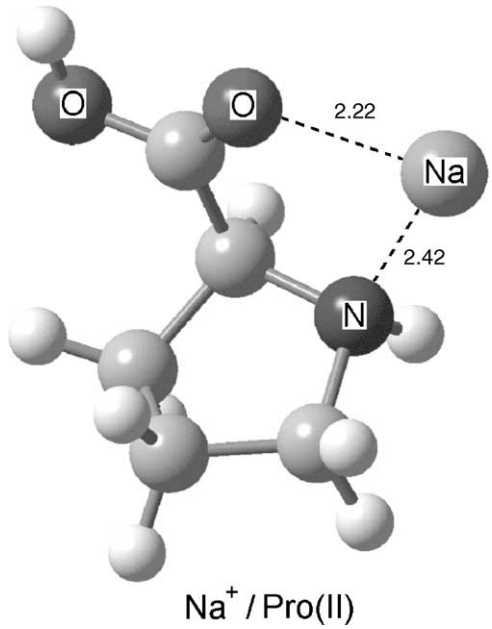

Fig. 8. Structure computed for the most stable conformer of the non-zwitterionic ProNa$^+$ complex.

stable by 58 kJ mol^{-1} than the N$^{\varepsilon 2}$-chelated isomer, which is shown in Fig. 9.

The assignment was made in Ref. [16] of two close low-lying conformers of PheNa$^+$. This system was not

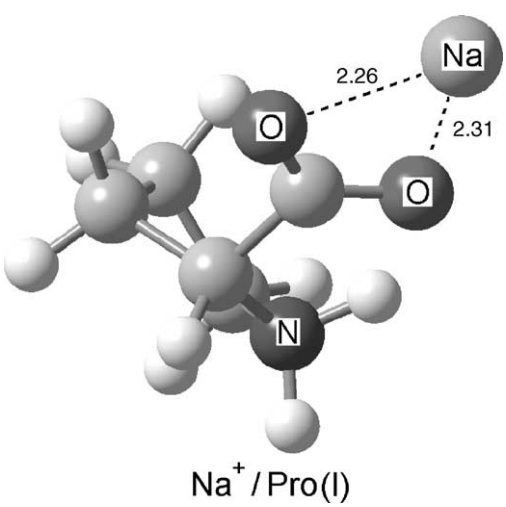

Fig. 7. Structure computed for the zwitterionic ProNa$^+$ complex, which is the most stable complexed form.

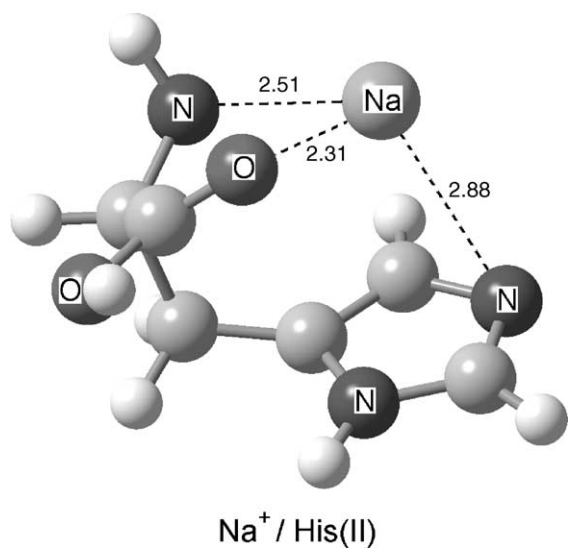

Fig. 9. Structure computed for the HisNa$^+$ complex in the less stable N$^{\varepsilon 2}$ tautomeric form.

investigated further here, beyond a recalculation of the energy of the complex with the present computational protocol.

4. Results and discussion

Table 6 summarizes the present experimental results relative to Ala, and puts them in context with some other recent work on the relative affinity scale for amino acids. For Gly and Cys, there is excellent agreement among the present experimental results, the kinetic method results, and the theoretical predictions. For Val, agreement between the experimental results is also excellent, while we have no recent theoretical results for comparison. For Phe, the experimental agreement is also excellent and agrees acceptably well with the computed values. The present experimental result for Ser is a bit lower than the kinetic method result (although the agreement is acceptable within experimental errors), and is also a bit below the low end of the range of computational results. The computed value (MP2 without BSSE correction) for Ser from Ref. [1] seems rather high in view of the two experimental values. The experimental values for Trp are in good accord, and also agree acceptably well with the computational results of Refs. [1,16]. The spread of experimental and computational results for Trp is somewhat larger than for the smaller molecules, but given the size and complexity of this molecule, the accord among the available numbers seems reasonably satisfactory.

Thus, for Gly, Val, Ser, Cys, Phe, and Trp, the conclusion from Table 6 is that the Na^+ affinities relative to Ala are under good experimental and theoretical control. The other three cases in the table have points of significant disagreement and interest. We will discuss these three cases in turn.

It is unfortunate that no equilibrium could be achieved here for Asn, since the kinetic method result and the present computation are in substantial disagreement. No resolution of this discrepancy is offered here.

Table 6
Na^+ affinities vs. Ala (enthalpies of transfer from the amino acid to Ala, kJ mol^{-1})

	Present experiments[a]	Present computations	Kinetic method[b]	Literature experiments	Literature computations
Gly	−8.1	−6.5	−5.7	−6[c]	−5.9[b], −3[d]
Ala	–	–	–	–	–
Val	4.0		6.4	7[c]	
Cys	9.6	4.3	8.4		9.4[b], 13[d]
Pro	6.5	23.1(−4.2)[e]	29.3		22.6[b], 28[d](0)[e,f]
Asn	(>7.3)[g]	19.7	38.9		
Ser	18.6	20.0	24.8		23.6[b], 33[d]
His	15.5	59.5(1.3)[h]	51.7		
Phe	28.8	22.1	31.6		25.9[b], 30.5[i]
Trp	35.8	48.7	42.9		

[a] Uncertainties relative to Ala are generally estimated as ±6 kJ mol^{-1}, although the relative uncertainties are probably less than this for Gly and Val, and greater than this for Phe and Trp.

[b] Ref. [13]. B3LYP/6-311+g(3df,2p)//B3LYP/6-31g(d).

[c] Ref. [19]. Kinetic method.

[d] Ref. [1]. Calculations used MP2/6-311+g(2d,2p)//MP2/6-31g* (without BSSE correction).

[e] Values in parentheses assume the most stable non-zwitterion structure for the complex.

[f] Non-zwitterion isomer of the complex. The isomer differential between zwitterion and non-zwitterion forms from Ref. [20] was combined with the Pro/Ala differential for the Pro zwitterionic complex from Ref. [1].

[g] Lower limit. Equilibrium was not established.

[h] The value in parentheses represents binding to the $N^{\delta 1}$–H tautomer of the neutral, which is much less favorable than binding to the $N^{\varepsilon 1}$–H tautomer.

[i] Ref. [8].

Pro is an interesting case. The present experimental result is completely out of line with both theory and with the kinetic method result. However, Pro is unique among these molecules in that the most stable structure of the Na^+ complex is the sodiated zwitterion (Fig. 7), while the neutral molecule strongly favors the non-zwitterionic structure. It appears that the equilibrium ligand attachment must proceed without rearrangement of the neutral to the zwitterionic form. This is strongly supported by the calculated range of relative binding energies for the non-zwitterionic complex between 0 and $-4\,kJ\,mol^{-1}$, which is in acceptable agreement with the present observed result of $6.5\,kJ\,mol^{-1}$.

The structure in Fig. 8, which is the lowest energy non-zwitterionic complex, can only rearrange to the zwitterionic complex (Fig. 7) by a major structural reorganization, and at the same time it is immediately formed by Na^+ attachment to the most stable conformer of neutral Pro. Thus, it makes sense to suppose that the equilibrium attachment–detachment process of Na^+ on Pro accesses only non-zwitterionic structures, and does not communicate with the zwitterion structures, at least on the time scale of these experiments. This is thus a believable picture that is consistent with the thermochemical results.

The pre-formed sodium heterodimer complexes used in the kinetic method work with Pro [1] probably had the complexed Pro ligand in zwitterionic form, since they were sprayed from aqueous solution, and accordingly it would be expected to show the higher dissociation energy necessary to detach the zwitterionic ligand, corresponding to the calculated relative values between 22 and $28\,kJ\,mol^{-1}$. Indeed, their result is in acceptable agreement with these calculations. Kish et al. did not establish the nature of the neutral fragment resulting from detachment of neutral Pro from the heterodimers. The agreement of their observed value with the expected zwitterion-to-non-zwitterion detachment process suggests that this rearrangement does take place during the detachment from their heterodimer complexes.

A large discrepancy is observed for His between the present results and the values from both theory and the kinetic method experiment (which are in reasonable accord). The origin of this discrepancy is not known, but it could possibly be related to the existence of two tautomers of His. In the zwitterionic form observed in condensed phase, the $N^{\varepsilon 1}$–H tautomer is much more stable than the $N^{\delta 1}$–H tautomer (using the terminology of Ref. [17]), although both tautomers are observed [17]. The non-zwitterionic form is more stable in the gas phase (and in fact, we calculate that the $N^{\varepsilon 1}$–H zwitterion tautomer reverts without barrier to the non-zwitterion form), but the relative energies of the two non-zwitterionic tautomers appear not to be experimentally known. At the present level of theory, the two tautomers of the non-zwitterionic neutral are calculated to have equal energies. Within the uncertainty of the calculation, the gas-phase mixture of tautomers could have either form predominant, or both present in comparable amounts.

Only the $N^{\varepsilon 1}$–H tautomer affords a favorable geometry for chelation of the Na^+ (Fig. 5). The $HisNa^+$ complex of the $N^{\delta 1}$–H tautomer (Fig. 9) is less stable by about $58\,kJ\,mol^{-1}$ than the complex of the $N^{\varepsilon 1}$–H tautomer (see Table 6). We speculate that the vapor of neutral His might consist predominantly of the $N^{\delta 1}$–H tautomer, and that interconversion of the tautomers is not possible on the experimental time scale. In that case, the Na^+ affinity of His observed in the present experiment would be that of the $N^{\delta 1}$–H tautomer. The calculated affinity of this tautomer ($1.3\,kJ\,mol^{-1}$ relative to Ala) is not in perfect agreement with the observed equilibrium result ($15.5\,kJ\,mol^{-1}$ from Table 6), but the agreement is far better than for the $N^{\varepsilon 1}$–H tautomer ($59\,kJ\,mol^{-1}$). This highly speculative scenario could explain the much lower equilibrium affinity of His in the present results compared with the kinetic method result.

4.1. Computational comparisons

The different computational approaches in use still give a substantial spread of predicted Na^+ affinities for most of the amino acids. Some representative recent values are noted in the tables. Judging by the limited survey of computational predictions shown in

Table 7
Comparison of experimental determinations of Na^+ affinity of glycine (kJ mol^{-1}, 298 K)

Value	Method	Reference
152 ± 9	Ligand exchange vs. Pyr	Present results[a]
161 ± 8	Kinetic method	Ref. [1]
166 ± 6	TCID	Ref. [18]
153 ± 10	TCID	Ref. [21]

[a] Value derived as the average of the value from present Gly experiment (151 kJ mol^{-1}) and our value for Ala (159 kJ mol^{-1}) from Ref. [8], assuming a differential of 6 kJ mol^{-1} between Gly and Ala. The anchor is Pyr (127.5 kJ mol^{-1}), for which Amunugama and Rodgers [22] give an uncertainty of 3 kJ mol^{-1}; this is combined with the uncertainty in our measurements to give the uncertainty of ±9 on our value.

Tables 6 and 8, in comparison with existing experimental results, no one computational approach seems to stand out as clearly more likely to agree with experiment.

The present DFT/B3P86 binding energies for Cys, Ser, and Phe are slightly lower than the DFT/B3LYP results in Ref. [13] using a comparable basis, and appear also to be too low in comparison with the experiments, although the differences are well within the experimental error and computational uncertainties. This might cast some slight doubt on the superiority of B3P86 over B3LYP for Na^+-binding calculations in these systems. The Pro values from the two DFT studies are very similar, but both appear low compared with the kinetic theory result, which is in better agreement with the MP2 value. The approach of MP2 without BSSE correction advocated in Refs. [1,18] consistently gives values slightly higher than DFT with a large basis and full BSSE correction. The experimental evidence is not sufficient to justify a preference for one or the other of these approaches.

Table 8
Absolute affinities (kJ mol^{-1}, 298 K where available)

	Present experiments[a]	Kinetic method[b]	Literature experiments	Present calculations	Literature calculations
Gly	161	161	153[c], 159[d] 166[e]	163	169.4[f], 164[b], 161[g], 155[h], 151[i]
Ala	169	167	165[d], 159[j]	169	175.3[f], 167[b], 170[k]
Val	173	173	172[d]		
Cys	179	175		173	184.7[f], 180[b], 168[i]
Pro	175	196		191[l], 164[l]	197.9[f], 195[b], 185[i]
Asn		206		188	
Ser	188	192		189	198.9[f], 200[b], 188[i]
His	185	219		226	
Phe	198	198	188[j], 174[m]	188	201.2[f], 201[k]
Trp	205	210	180[m]	217	218[k]
MeAla	176			176	
MeVal	179			180	

[a] Absolute uncertainties estimated as ±12 kJ mol^{-1}, including both uncertainties of individual determinations, and an overall uncertainty of ±8 kJ mol^{-1} in the anchoring of the affinity scale.
[b] Ref. [1]. Computations by MP2 (no BSSE). Experiments by kinetic method.
[c] Ref. [21]. TCID.
[d] Ref. [19]. Kinetic method (uncertain absolute anchor).
[e] Ref. [18]. TCID.
[f] Ref. [13]. DFT/B3LYP.
[g] Ref. [18]. MP2 (no BSSE).
[h] Ref. [18]. CBS-QB3.
[i] Ref. [20]. MP2 (full BSSE).
[j] Ref. [8]. Equilibrium ligand transfer.
[k] Refs. [8,16]. DFT/B3P86.
[l] First value is for zwitterionic complex, second value is for non-zwitterionic complex.
[m] Ref. [23]. Kinetic method.

4.2. Absolute Na^+ affinities

The absolute anchoring of the affinity scale remains somewhat uncertain, because credible computational and experimental values of absolute affinities scatter over a range of more than $\pm 10\,kJ\,mol^{-1}$. We can note here four relatively recent experimental assignments of the Na^+ affinity of Gly, as shown in Table 7, having a range of $14\,kJ\,mol^{-1}$. In addition to the present results and the kinetic method results previously noted, the table also includes two careful determinations using the threshold collision-induced dissociation (TCID) technique. Theoretical values will not be reviewed in detail here. They scatter over an even wider range of absolute values than the experimental results, and give little useful guidance to the correct anchoring of the scale (see Ref. [18] for a recent discussion of both computed and experimental values).

The agreement for these experimental results is not perfect, seeming to confirm that the uncertainties quoted by the various groups did not overestimate the uncertainties of their experiments. The value of $161\,kJ\,mol^{-1}$, which was adopted by Kish et al., is within the range of uncertainty of all four measurements, and can be taken as our best current estimate of the anchoring of the affinity scale. They gave an uncertainty of $\pm 8\,kJ\,mol^{-1}$ to this anchor, and we consider this to be a realistic estimate of the uncertainty in the absolute level of this affinity scale.

Given this anchor, we can give absolute affinities derived from the present experiments, as shown in Table 8. With the exceptions already discussed, the experimental values and recent theoretical values are generally in satisfactory accord.

5. Conclusion

The present Na^+ affinity measurements give a satisfactory picture of the affinity scale for Gly, Ala, Val, Cys, Ser, Phe, and Trp. Agreement with other experiments is acceptable, and often excellent. Agreement with computations is satisfactory, although the precision of the experimental determinations is still not good enough for definitive evaluation of the different computational protocols currently in use. The absolute anchoring of the affinity scale at $161\,kJ\,mol^{-1}$ for Gly seems secure within a rather large uncertainty range of $\pm 8\,kJ\,mol^{-1}$.

Three anomalous cases emerged from the present study. The best understood of these is Pro, where the affinity from the present ligand transfer study is significantly lower than the ligand detachment energy derived from the kinetic method work. It seems likely that the equilibrium Na^+ attachment to neutral Pro never accesses the more stable zwitterionic form of the complex, and that the affinity measured by ligand attachment reflects the energy of the less stable non-zwitterionic complex (Fig. 8). This is an interesting illustration of basic differences between ligand-attachment strategies as opposed to complex-dissociation strategies for the determination of binding energies of ion complexes.

The present calculation of the $AsnNa^+$ complex predicts a substantially lower affinity that was observed by the kinetic method. Since we were not able to establish equilibrium for this system to make a measurement, and since we are not aware of other high-level computations of this system, we simply indicate this as a possible anomaly for future study.

The present experiments gave a much lower affinity for His than expected either from theory or from the kinetic method results. A very speculative explanation for this was offered, postulating that neutral His in the gas phase exists predominantly in the tautomeric form which is unfavorable to Na^+ complexation, and that it is the affinity of this tautomer that is observed in the ligand-attachment equilibrium.

Although equilibrium ligand exchange is experimentally more difficult and less broadly applicable than methods involving dissociation of pre-formed metal–ion complexes, the present work illustrates the importance of this complementary approach to thermochemistry and ion-binding studies. The good agreement of the present results with the dissociative results for most of the amino acids gives an independent solidification of the thermochemical picture. The anomalous cases, both Pro and His, point to

situations where the existence of multiple tautomers and zwitterions may lead to complications in the thermochemistry that are not immediately evident in the simple dissociation of electrosprayed complexes. These anomalous cases are not yet definitively understood, and it is clear that there is more there to think about. Finally, while it was not realized in the present work, the prospect of a fully temperature-resolved equilibrium measurement of a key amino acid like Ala against a well-understood reference ligand will eventually allow direct measurements of the entropy contributions to the free energy of ion attachment. This will lead to an absolute anchoring of the affinity scale of these chelating ligands with greater accuracy and confidence than can be given by any other non-spectroscopic method.

Acknowledgements

This work benefited from the support of the donors of the Petroleum Research Fund, administered by the American Chemical Society.

References

[1] M.M. Kish, G. Ohanessian, C. Wesdemiotis, Int. J. Mass Spectrom. (2003) in press.
[2] T.B. McMahon, G. Ohanessian, Chem. Eur. J. 6 (2000) 2931.
[3] P.D. Godfrey, S. Firth, L.D. Hatherley, R.D. Brown, A. Pierlot, J. Am. Chem. Soc. 115 (1993) 9687.
[4] K. Ijima, B. Beagley, J. Mol. Struct. 248 (1991) 133.
[5] T.P. Debies, J.W. Rabalais, J. Electron Spectrosc. Relat. Phenom. 3 (1974) 315.
[6] R. Antoine, I. Compagnon, D. Rayane, M. Broyer, P. Dugourd, G. Breaux, F.C. Hagemeister, D. Pippen, R.R. Hudgins, M.F. Jarrold, Eur. Phys. J. D 20 (2002) 583.
[7] A. Gapeev, C.-N. Yang, S.J. Klippenstein, R.C. Dunbar, J. Phys. Chem. A 104 (2000) 3246.
[8] A. Gapeev, R.C. Dunbar, J. Am. Chem. Soc. 123 (2001) 8360.
[9] P.B. Armentrout, M.T. Rodgers, J. Phys. Chem. A 104 (2000) 2238.
[10] S.S. Xantheas, J. Chem. Phys. 104 (1996) 8821.
[11] S. Gronert, R.A.J. O'Hair, J. Am. Chem. Soc. 117 (1995) 2071.
[12] A.G. Császár, J. Phys. Chem. 100 (1996) 3541.
[13] F.M. Siu, Ph.D. Thesis, Hong Kong Polytechnic University, 2001.
[14] A.G. Császár, J. Am. Chem. Soc. 114 (1992) 9568.
[15] A.G. Császár, A. Perczel, Prog. Biophys. Mol. Biol. 71 (1999) 243.
[16] R.C. Dunbar, J. Phys. Chem. A 104 (2000) 8067.
[17] S. Farr-Jones, W.Y.L. Young, W.G. Gutheil, W.W. Bachovchin, J. Am. Chem. Soc. 115 (1993) 6813.
[18] R.M. Moision, P.B. Armentrout, J. Phys. Chem. A 106 (2002) 10350.
[19] G. Bojesen, T. Brendahl, U. Anderson, Org. Mass Spectrom. 28 (1993) 1448.
[20] S. Hoyau, K. Norrman, T.B. McMahon, G. Ohanessian, J. Am. Chem. Soc. 121 (1999) 8864.
[21] J.S. Klassen, S.G. Andersen, A.T. Blades, P. Kebarle, J. Phys. Chem. 100 (1996) 14218.
[22] R. Amunugama, M.T. Rodgers, Int. J. Mass Spectrom. 195/196 (2000) 439.
[23] R.C. Dunbar, V. Ryzhov, B.A. Cerda, C. Wesdemiotis, J. Am. Soc. Mass Spectrom. 11 (2000) 1037.